Fast vibrational calculation of anharmonic OH-stretch frequencies for two low-energy noradrenaline conformers

David M. Benoit[a)]
Nachwuchsgruppe Theorie-SFB 569, Albert-Einstein-Allee 11, University of Ulm, D-89081 Ulm, Germany

(Received 26 September 2008; accepted 13 November 2008; published online 16 December 2008)

We introduce a new reduced-coupling technique to accelerate direct calculations of a selected number of vibrational frequencies in large molecular systems. Our method combines the advantages of the single-to-all correlation-corrected vibrational self-consistent field (STA-CC-VSCF) approach [D. M. Benoit, J. Chem. Phys. **125**, 244110 (2006)] with those of the fast-CC-VSCF technique [D. M. Benoit, J. Chem. Phys. **120**, 562 (2004)] and allows the *ab initio* calculation of only the relevant parts of the required potential energy surface (PES). We demonstrate, using a set of five aliphatic alcohol molecules, that the new fast-STA-CC-VSCF method is accurate and leads to very substantial time gains for the computations of the PES. We then use the fast-STA-CC-VSCF method to accelerate the computation of the OH-stretch and NH-stretch frequencies of the two lowest-energy conformers of noradrenaline, namely, AG1a and GG1a. Our new approach enables us to run the calculation 89 times faster than the standard CC-VSCF technique and makes it possible to use a high-level MP2/TZP description of the PES. We demonstrate that the influence of the strong mode-mode couplings is crucial for a realistic description of the particular OH-stretch vibrational signature of each conformer. Finally, of the two possible low-energy conformers, we identify AG1a as the one most likely to have been observed in the experiments of Snoek *et al.* [Mol. Phys. **101**, 1239 (2003)]. © *2008 American Institute of Physics*. [DOI: 10.1063/1.3040427]

I. INTRODUCTION

Noradrenaline, also known as norepinephrine, has recently been the subject of extensive *ab initio* studies by van Mourik[1] and van Mourik and Früchtl.[2] These studies were initiated by the spectroscopic observations of Snoek *et al.*,[3] who managed to vaporize noradrenaline without any decomposition using a laser desorption technique. They recorded a series of mass-selected ion-dip spectra that provides an interesting perspective on the vibrational dynamics of this catecholamine. Moreover, they used hole-burning spectroscopy to establish that the spectra recorded originated from a single conformer. However, as is the case for most large biomolecules, the conformer assignment relied on a harmonic analysis based on *ab initio* calculations.

Van Mourik's study[1] suggested that the original harmonic analysis used by Snoek *et al.* to determine the nature of the conformer observed experimentally is potentially flawed. Indeed, van Mourik's harmonic analyses performed at a higher level of *ab initio* theory than that of Ref. 3 reveal that the vibrational frequencies of the two low-energy conformers of noradrenaline (AG1a and GG1a) are nearly identical, thus making it impossible to unequivocally assign the observed transition frequencies on the basis of harmonic calculations alone. Moreover, MP2 and df-LMP2 calculations using up to quadruple-zeta basis sets[1] reveal that the energy difference between AG1a and GG1a is very small (below 1 kcal/mol), and demonstrate that the relative isomer energetic ordering depends strongly on the level of theory and basis set used. This suggests that the two conformers are degenerate at these levels of theory and thus renders an assignment on the basis of energetic criteria virtually impossible. Attempts to determine the difference in Gibbs free energy for these two conformers[1,4] have remained inconclusive, but have highlighted the importance of anharmonic corrections.

Given the delicate balance of forces at play in each conformer and the insights provided by the torsional path-integral Monte Carlo study by Miller III and Clary[4] on the closely related adrenaline molecule, we expect anharmonic effects to be an important factor in the vibrational dynamics of both the extended AG1a conformer and the more compact GG1a conformer. Consequently, going beyond a harmonic description of the vibrations in noradrenaline should provide a suitable basis for understanding the vibrational signature of each conformer.

The vibrational self-consistent field (VSCF) method provides an accurate way of solving the vibrational Schrödinger equation beyond the harmonic model for large molecules, particularly when mode-mode correlation is taken into account using perturbative correlation corrections (CC-VSCF).[5,6] This approach, also known as vibrational Møller–Plesset perturbation theory,[7,8] is the most straightforward correlation-correction technique. Other alternatives, such as vibrational configuration interaction[9,10] (VCI) or vibrational coupled cluster[11] do exist, but require significantly more computational resources for large systems. In the case of noradrenaline, van Mourik's study[1] showed that a high level of *ab initio* theory is necessary to describe the potential energy surface (PES) of these conformers correctly and, therefore, given the size of this system, a standard CC-VSCF

[a)]Electronic mail: david.benoit@uni-ulm.de.

calculation cannot be performed in a reasonable computational time.

To address this issue, we introduce in this paper a new method that combines our recently developed single-to-all CC-VSCF (STA-CC-VSCF) (Ref. 12) technique with the fast-CC-VSCF method.[6] We demonstrate, using a series of aliphatic alcohol molecules, that this new method is of similar accuracy to a fast-CC-VSCF calculation but can also be used advantageously for large systems in order to reduce the number of mode-mode coupling potential energy terms required for the CC-VSCF technique.

We then use our new fast-STA-CC-VSCF method to compute the OH-stretch region of the spectra for AG1a and GG1a conformers of noradrenaline in order to elucidate the attribution of the bands observed in the 2500–3500 cm^{-1} region by Snoek *et al.*[3]

The outline of this paper is as follows. In Sec. II, we first give a brief description of the VSCF technique and the correlation-correction method used in this study. We then describe in detail the fast-STA approximation. Further computational details are given in Sec. III. In Sec. IV, we investigate the efficiency and accuracy of our new scheme for the prediction of OH-stretch frequencies of aliphatic alcohol molecules. We then present a practical solution to the problem of normal-mode matching that can occur in fast-CC-VSCF calculations, and apply our new technique to compute the anharmonic vibrational spectra of two noradrenaline isomers. Finally, we present our conclusions in Sec. V.

II. THEORY AND METHODS

A. Vibrational self-consistent field method and correlation correction

Since the VSCF technique has been extensively described elsewhere,[13,14] we only highlight here the main features of this method. The vibrational Schrödinger equation for the molecular system investigated is expressed in mass-weighted normal coordinates $\mathbf{Q} \equiv \{Q_1, Q_2, \ldots, Q_N\}$ as

$$\left\{ -\frac{1}{2}\sum_{j=1}^{N} \frac{\partial^2}{\partial Q_j^2} + V(\mathbf{Q}) \right\} \Psi_{\mathbf{n}}(\mathbf{Q}) = E_{\mathbf{n}} \Psi_{\mathbf{n}}(\mathbf{Q}), \tag{1}$$

where $V(\mathbf{Q})$ is the full PES of the N-dimensional problem, and $\mathbf{n} \equiv \{n_1, n_2, \ldots, n_N\}$ is a collective index representing the excitation quanta of the vibrational wave function. Note that we neglect the Coriolis coupling term of the molecular Hamiltonian since the error arising from ignoring this term decreases as the size of the molecular system increases.[15]

The total wave function is expressed as a separable product of normal coordinate functions

$$\Psi_{\mathbf{n}}(\mathbf{Q}) = \prod_{j=1}^{N} \varphi_{n_j}^{(\mathbf{n})}(Q_j), \tag{2}$$

which leads to N one-dimensional VSCF equations,

$$\left\{ -\frac{1}{2}\frac{\partial^2}{\partial Q_j^2} + V_j^{(1)}(Q_j) + \vartheta_j^{(\mathbf{n})}(Q_j) \right\} \varphi_{n_j}^{(\mathbf{n})}(Q_j) = \epsilon_{n_j}^{(\mathbf{n})} \varphi_{n_j}^{(\mathbf{n})}(Q_j). \tag{3}$$

These equations are coupled together through a mean-field potential,

$$\vartheta_j^{(\mathbf{n})}(Q_j) = \left\langle \varphi_{n_i}^{(\mathbf{n})} \prod_{i \neq j}^{N} \middle| V_c(\mathbf{Q}) \middle| \prod_{i \neq j}^{N} \varphi_{n_i}^{(\mathbf{n})} \right\rangle, \tag{4}$$

where $V_c(\mathbf{Q})$ contains all the coupling terms of the potential energy operator and $V_j^{(1)}(Q_j)$ represents the diagonal part of the potential associated with mode j. Equations are resolved self-consistently until convergence of the total VSCF energy given by

$$E_{\mathbf{n}} = \sum_{j=1}^{N} \epsilon_{n_j}^{(\mathbf{n})} - (N-1) \left\langle \varphi_{n_j}^{(\mathbf{n})} \prod_{j=1}^{N} \middle| V_c(\mathbf{Q}) \middle| \prod_{j=1}^{N} \varphi_{n_j}^{(\mathbf{n})} \right\rangle. \tag{5}$$

The PES, $V(\mathbf{Q})$, is described by an N-body representation[5,16–18]

$$V(\mathbf{Q}) = \sum_{j=1}^{N} V_j^{(1)}(Q_j) + \sum_{i=1}^{N} \sum_{j>i}^{N} V_{ij}^{(2)}(Q_i, Q_j) + \sum_{i=1}^{N} \sum_{j>i}^{N} \sum_{k>j}^{N} V_{ijk}^{(3)}(Q_i, Q_j, Q_k) + \ldots. \tag{6}$$

Chaban *et al.* showed that a pairwise approximation of the PES coupled to a correlation-corrected VSCF scheme is sufficient to give reasonable vibrational frequencies for large molecular systems,[19] while greatly simplifying the evaluation of the integrals needed for the calculation of the effective potential. The contribution of the remaining higher-order terms in Eq. (6) is small but not negligible;[20–22] nevertheless, the inclusion of such terms in the PES incurs a large additional computational cost. Thus, in this work, we use an approximation to Eq. (6) that includes in the PES only terms up to second order in V, that is, a series of diagonal terms, $V_j^{(1)}(Q_j)$, and a series of mode-mode coupling terms, $V_{ij}^{(2)}(Q_i, Q_j)$.

Since the VSCF scheme uses a mean-field potential to account for mode-mode coupling, a perturbative approach based on second-order Møller–Plesset perturbation theory was proposed by Norris *et al.*[23] Later, Matsunaga *et al.*[24] extended this method to deal with degenerate vibrational states and, more recently, Yagi *et al.*[25] suggested a quasidegenerate perturbation technique. The nondegenerate perturbation method uses the VSCF vibrational wave functions and their zero-order eigenvalues to compute the second-order correction for the energy of vibrational configuration $|\Psi_{\mathbf{n}}\rangle$,

$$E_{\mathbf{n}}^{\mathrm{CC}} = E_{\mathbf{n}}^{\mathrm{VSCF}} + \sum_{\mathbf{m}\neq\mathbf{n}} \frac{|\langle\Psi_{\mathbf{n}}|\hat{\mathbf{H}} - \hat{\mathbf{H}}_0|\Psi_{\mathbf{m}}\rangle|^2}{E_{\mathbf{n}}^{(0)} - E_{\mathbf{m}}^{(0)}} \quad \text{with} \quad E_{\mathbf{n}}^{(0)} = \sum_{j=1}^{N} \epsilon_{n_j}^{(\mathbf{n})}, \tag{7}$$

where $\hat{\mathbf{H}}_0$ is the VSCF effective Hamiltonian optimized for vibrational configuration $|\Psi_{\mathbf{n}}\rangle$. The main advantage of this CC-VSCF perturbative scheme is its low computational cost, which makes it suitable for large molecular systems. We note, however, that perturbative schemes can sometimes lead to nonphysical corrections, as reported by Chaban[19] and Christiansen.[7]

B. Fast-single-to-all method

We have recently introduced a method that enables fast and accurate calculations of selected vibrational frequencies in a molecule within the framework of correlation-corrected VSCF.[12] This method, called STA-CC-VSCF, has a formal computational scaling of $N \cdot N_{\mathcal{A}}$ for the computation of the necessary PES for $N_{\mathcal{A}}$ selected vibrational modes among N modes present in the system. This approach divides the normal modes $\mathbf{Q}$ into two groups. The first group, $\mathbf{Q}^{\mathcal{A}}$, contains all the active modes present in the observed vibrational spectra (for example, in the case of a single OH-stretch, $N_{\mathcal{A}}=1$). The rest of the $N_{\mathcal{I}}=N-N_{\mathcal{A}}$ normal modes form the second group, $\mathbf{Q}^{\mathcal{I}}$, and are treated as uncoupled anharmonic modes. This partitioning leads to the following expression for the PES:

$$V(\mathbf{Q}) = \sum_{i=1}^{N_{\mathcal{A}}} V_i^{\mathcal{A},(1)}(Q_i^{\mathcal{A}}) + \sum_{j=1}^{N_{\mathcal{I}}} V_j^{\mathcal{I},(1)}(Q_j^{\mathcal{I}}) + \sum_{i=1}^{N_{\mathcal{A}}} \sum_{j>i}^{N_{\mathcal{A}}} V_{ij}^{\mathcal{A}\mathcal{A},(2)}(Q_i^{\mathcal{A}}, Q_j^{\mathcal{A}}) + \sum_{i=1}^{N_{\mathcal{A}}} \sum_{j=1}^{N_{\mathcal{I}}} V_{ij}^{\mathcal{A}\mathcal{I},(2)}(Q_i^{\mathcal{A}}, Q_j^{\mathcal{I}}). \tag{8}$$

For $N_{\mathcal{A}} \ll N$, the computational scaling of the vibrational part of the calculation following the generation of the PES is close to $N^{4.5}$, two orders of magnitude smaller than standard CC-VSCF computations. The reduction in the computational scaling is obtained by using a screened version of the correlation-correction term, which constitutes the bottleneck of the *vibrational* calculation (see Ref. 12 for details). Note that the STA approach can also be extended to the VCI method,[26] leading to noticeable speed improvements for VCI calculations.

However, for a system containing a large number of normal modes N, the computation of $(N-1)N_{\mathcal{A}}$ coupling elements, as required by the second-order expansion of the PES shown in Eq. (8), can be time consuming. We have demonstrated previously[6] that a careful selection of the mode-mode coupling parts of the PES (fast-CC-VSCF) leads to a significant acceleration in the PES construction without introducing any major error into the CC-VSCF computation. Consequently, we suggest applying the fast-CC-VSCF technique to the $(N-1)N_{\mathcal{A}}$ coupling elements to reduce their number by keeping only the most significant contributions to the PES for the selected $N_{\mathcal{A}}$ modes. The selection technique developed for fast-CC-VSCF can be easily applied here by defining the following measure of mode-mode coupling strength for each couple of modes:

$$\zeta(Q_i, Q_j) = \frac{1}{N_{\mathrm{grid}}^2} \sum_{n_i=1}^{N_{\mathrm{grid}}} \sum_{n_j=1}^{N_{\mathrm{grid}}} |V_{ij}^{(2)}(n_i, n_j)|, \tag{9}$$

where n_i and n_j are the sampled points for each normal mode Q_i and Q_j, respectively, and N_{grid} is the total number of grid points for each normal mode (usually 16 points). The PES used for the computation of the ζ values is typically obtained using an approximate electronic structure theory, for example the semiempirical PM3 Hamiltonian. The ij mode-mode couplings retained in the fast-STA calculation are the ones whose $\zeta(Q_i, Q_j)$ value is greater than a threshold value $\zeta_{\mathrm{threshold}}$. The selected mode-mode couplings are then recomputed using a high-level electronic structure method while the other couplings are neglected. In this work, we set $\zeta_{\mathrm{threshold}} \approx 0.2 \max[\zeta(Q_i, Q_j)]$, and, as with the STA-CC-VSCF method, we use a screening scheme for the correlation-correction part of the CC-VSCF algorithm.[12]

III. COMPUTATIONAL DETAILS

All the calculations necessary for the generation of PESs are performed using the GAMESS-US package.[27] For each system, we first perform a full geometry optimization at the chosen level of *ab initio* theory. Harmonic frequencies and normal-mode coordinates are then computed by a double-difference scheme using analytical gradients for the equilibrium geometry obtained. The PESs used are computed at the MP2 level of theory, and we use the pseudopotential basis developed by Stevens and co-workers (SBK),[28–30] augmented by a set of polarization functions, and the triple-zeta basis set (TZP) of Dunning[31] with polarization functions. For the TZP basis set, the MP2 calculations are performed using the frozen-core approximation.

The VSCF routine evaluates the *ab initio* potential energy along each normal coordinate Q_i using a fixed number of points for each diagonal anharmonicity term and a grid of points for each mode–mode coupling term. These points form a discretized version of the PES of the system $V(\mathbf{Q})$, as formulated in Eq. (6). The self-consistent vibrational calculation is then performed, and includes a perturbative correction of the coupling between modes as described by Eq. (3) and Eq. (7). We choose to use 16 regularly spaced points to represent the diagonal potential energy curve along each normal mode, $V_j^{(1)}(Q_j)$, in Eq. (6), and to calculate the second-order pair-coupling potentials, $V_{ij}^{(2)}(Q_i, Q_j)$, on a set of 256 regular grid points (16×16). In this paper, the results indicated by "full" are obtained using the standard direct CC-VSCF method as implemented in the GAMESS-US computer program, version 7 SEP 2006 (R4), while the other results are obtained with our locally modified version of the GAMESS-US package. All calculations are performed on a cluster of Apple Xserve G5 computers.

TABLE I. Computed vibrational frequencies of the OH-stretch of aliphatic alcohols of varying carbon-chain length using an MP2/SBK(d,p) PES (see Ref. 12 for details); comparison of direct full CC-VSCF (*full*), with direct STA-CC-VSCF (*STA*), direct fast-CC-VSCF (*fast*), and direct fast-STA-CC-VSCF (*fast-STA*). Deviation from full CC-VSCF results are shown in parentheses; all frequencies are in cm^{-1}. Representative timings for the computation of the PES (t_{rel}^{PES}) in each case are relative to methanol for a full CC-VSCF calculation.

	Methanol		Ethanol		*n*-propanol		*n*-butanol		*n*-pentanol	
	$\tilde{\nu}_{OH}$	t_{rel}^{PES}	$\tilde{\nu}_{OH}$	t_{rel}^{PES}	$\tilde{\nu}_{OH}$	t_{rel}^{PES}	$\tilde{\nu}_{OH}$	t_{rel}^{PES}	$\tilde{\nu}_{OH}$	t_{rel}^{PES}
Full	3644	1.0	3623	11.9	3621	64.7	3613	246.3	3610	976.9
STA	3639 (−5)	0.2	3622 (−1)	1.4	3620 (−1)	5.6	3614 (+1)	19.2	3609 (−1)	43.2
Fast	3648 (+4)	0.2	3629 (+6)	1.0	3641 (+20)	4.2	3640 (+27)	16.1	3639 (+29)	33.8
Fast-STA	3647 (+3)	0.1	3631 (+8)	0.4	3631 (+10)	1.6	3627 (+14)	4.9	3626 (+16)	8.5

IV. RESULTS

A. Computational efficiency and accuracy of the method

In order to assess the computational efficiency and the accuracy of the fast-STA-CC-VSCF method, we perform a series of calculations of the OH-stretch frequency for the five simple aliphatic alcohols investigated in our previous STA-CC-VSCF study,[12] namely methanol to *n*-pentanol. We use the mode-mode coupling map obtained from our earlier STA-CC-VSCF investigation and include in the fast-STA-CC-VSCF calculation only mode–mode couplings for which $\zeta \geq 0.2\zeta_{max}$. The results obtained for a PES computed at an MP2/SBK(d,p)level of theory are summarized in Table I, along with standard CC-VSCF, STA-CC-VSCF, and fast-CC-VSCF results for comparison.

We observe that the vibrational frequencies computed using the fast-STA-CC-VSCF method are closer to the full CC-VSCF or the STA-CC-VSCF method than to those obtained with a fast-CC-VSCF calculation. There is, however, a deviation between the fast-STA and the STA results that increases slightly with system size. This deviation is expected since the PES used in the fast-STA method contains only the most important mode-mode couplings and neglects the smaller coupling contributions (see, for example, the coupling maps for methanol in Fig. 1). Note that such size-dependent deviation is also observed, in larger proportions, for the fast-CC-VSCF results. Nevertheless, the agreement between fast-STA-CC-VSCF results and STA-CC-VSCF results (or similarly between those of fast-CC-VSCF and full CC-VSCF) can be improved at will by decreasing the selection threshold at the expense of computer time during

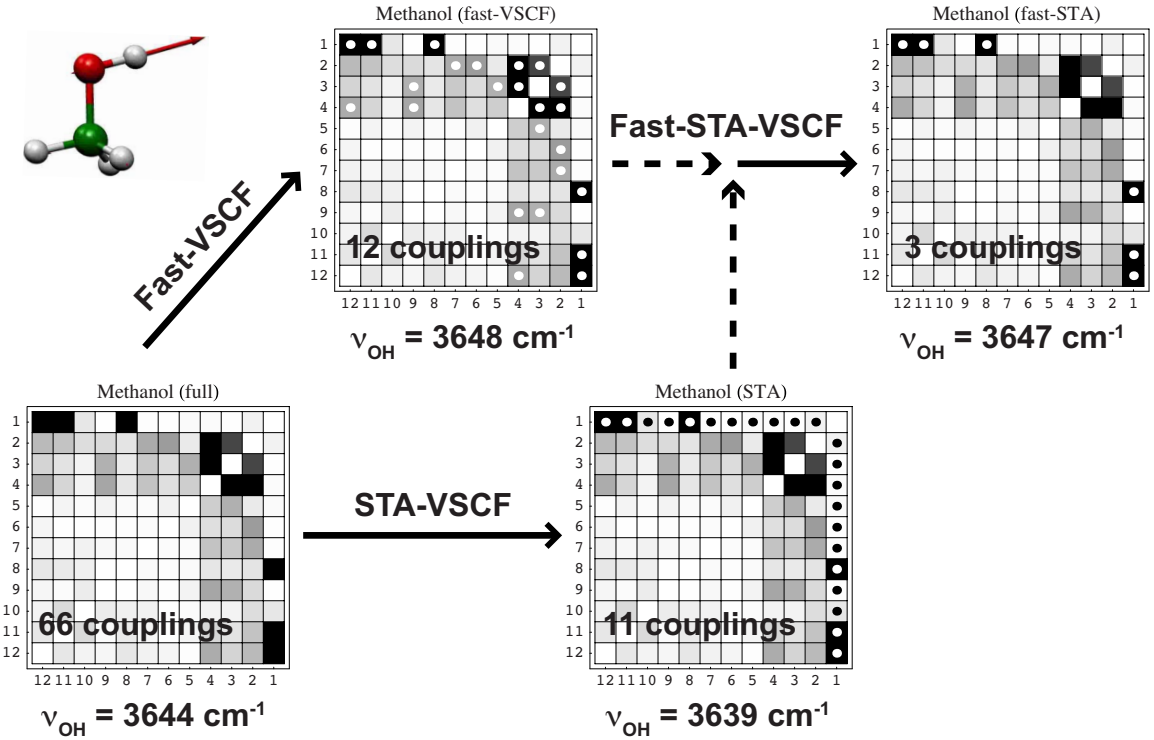

FIG. 1. (Color online) Series of mode-mode coupling maps for the methanol molecule showing the relationship between full, fast, STA, and fast-STA approaches to CC-VSCF calculations. Each map is computed at the MP2/SBK(d,p) level of theory and shows the magnitude of the potential energy coupling ($V_{ij}^{(2)}$) for each pair of normal modes. Weaker couplings are represented by lighter-colored squares and stronger couplings by darker ones. Dots indicate the pair couplings included in a typical fast-CC-VSCF, STA-CC-VSF, or fast-STA-CC-VSCF calculation of the OH-stretch frequency (mode 1). The computed ν_{OH} frequency obtained for each approach is reported below its respective coupling map.

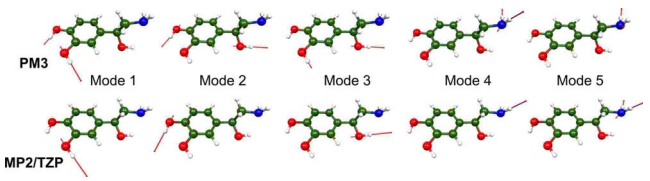

FIG. 2. (Color online) Graphical representation of the five highest-frequency normal modes of the AG1a conformer of noradrenaline. The modes shown on the top row were computed using the PM3 semiempirical Hamiltonian and those in the bottom row using MP2/TZP.

the calculation of the PES. The lower accuracy of the fast-CC-VSCF scheme compared to the fast-STA-CC-VSCF scheme is due to the different intended usage of each method. The fast-CC-VSCF approach aims to provide a *complete* vibrational spectrum, and therefore the coupling selection is performed over all mode-mode couplings ($[N(N-1)]/2$ elements). The fast-STA approach, on the other hand, aims at accelerating the computation of a *limited* number of vibrational frequencies and thus performs its coupling selection on an already reduced number of mode-mode couplings $[(N-1)N_{\mathcal{A}}$ elements].

The real advantage of the fast-STA approach resides in the drastic reduction in the computational time at the PES-construction stage of the CC-VSCF calculation. For example, the PES stage for the pentanol molecule is reduced by a factor close to 5 compared to a STA approach, by a factor of 4 compared to the fast-CC-VSCF method and by a factor of 115 compared to a full CC-VSCF calculation. Moreover, once the number of mode-mode couplings has been reduced using fast-STA, a further speed increase could be obtained by using fitting-based techniques[32,33] to reduce the number of points required for the calculation of each remaining coupling.

The frequency deviation that results from neglecting parts of the PES for this molecule is still relatively small (0.4% of the frequency) and is smaller than for the fast-CC-VSCF approach (0.8% of the frequency). We observe only a slight difference between the timings of the CC-VSCF vibrational stages of both the fast-STA and STA methods. Typically the fast-STA method is about 5% faster at the CC-VSCF vibrational stage than a STA-CC-VSCF calculation.

B. Low-level coupling determination

The original fast-CC-VSCF procedure requires the computation of a low-level PES around an optimized structure obtained at that same level of theory and using the corresponding normal modes as coordinates. Heislbetz *et al.*[34] recently investigated the impact of using low-level normal modes on the quality of composite multilevel PESs generated by combining coupled-cluster and MP2 results. They showed for small molecules up to seven atoms that the use of approximate normal modes has a negligible impact on the results of VSCF/VCI calculations performed on such multilevel surfaces.

However, for large systems, the molecular geometry can depend crucially on the actual level of electronic structure calculation used, and a full optimization at a lower level of theory can lead to large differences in the nature of the normal modes obtained. Figure 2 shows an example for the normal modes of the AG1a conformer of noradrenaline obtained at the PM3 and MP2/TZP levels of theory.

In the present case, the nature of the normal modes describing the OH-stretch region at the PM3 level is different from those obtained at the MP2/TZP level. We see that for PM3, modes 1, 2, and 3 are more delocalized than the MP2/TZP modes. The NH-stretch modes, modes 4 and 5, are of a similar nature for both levels of theory but are swapped around. Since direct vibrational calculations use normal modes as a coordinate system to construct the PES, the discrepancies between the levels of theory will lead to different regions of the PES being explored in each case. Moreover, this situation can lead to qualitative differences in the mode-mode coupling strength and to an additional mapping problem between low-level and high-level normal modes. Therefore, to circumvent this issue, we modify the original fast-CC-VSCF scheme and use exclusively the high-level molecular geometry and the corresponding normal modes to perform the preliminary low-level PES exploration. The mode-mode coupling patterns obtained for methanol using the original and this modified fast-CC-VSCF prescription are shown in Fig. 3.

We see in Fig. 3 that the coupling map obtained with PM3 is similar to the one obtained with MP2/SBK(d,p) but shows differences for several mode-mode coupling strengths

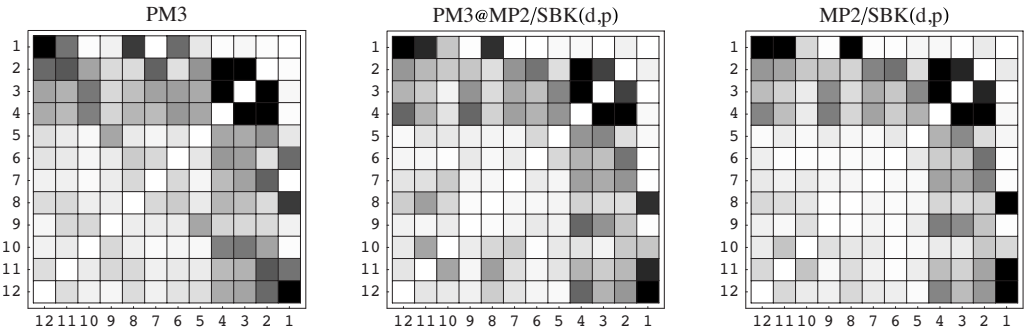

FIG. 3. Mode-mode coupling maps for the methanol molecule, showing the magnitude of the potential energy coupling ($V_{ij}^{(2)}$) for each pair of normal modes. The PM3 map (left) is computed using PM3 for a fully optimized geometry. The PM3 @ MP2/SBK(d,p) map (center) is computed using PM3 for a geometry optimized using MP2/SBK(d,p). The MP2/SBK(d,p) map (right) is computed using MP2/SBK(d,p) for a fully optimized geometry.

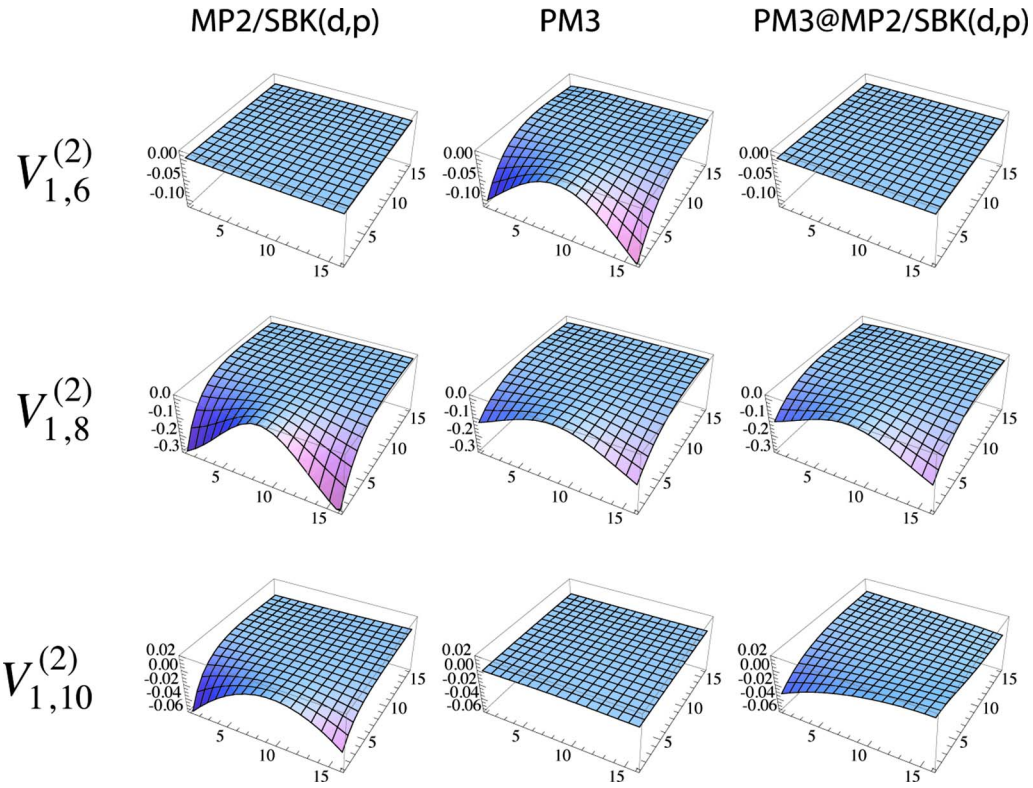

FIG. 4. (Color online) Selected mode-mode potential energy coupling ($V^{(2)}_{ij}$) as a function of grid-point numbers for the methanol molecule, computed at different levels of theory.

(see, for example, the coupling between modes 1 and 10 or 1 and 6). This is due to the difference between the underlying descriptions of the PES for each method, which leads to slightly different normal modes in each case. By using the normal modes obtained from an MP2/SBK(d,p) calculation to compute the coupling map with PM3, we obtain a better match for the full MP2/SBK(d,p) map. We note that the rms difference between the PM3 and MP2/SBK(d,p) coupling maps is 1.32, while those of the PM3 @ MP2/SBK(d,p) and MP2/SBK(d,p) coupling maps is 1.19, which is a 13% decrease in rms difference. The different nature of the PESs can be seen from the selected $V^{(2)}_{ij}$ elements shown in Fig. 4.

We observe that there are some qualitative differences between the coupling potential obtained at the MP2/SBK(d,p) and the PM3 levels of theory. For example, $V^{(2)}_{1,6}$ is relatively constant for MP2/SBK(d,p) and PM3 @ MP2/SBK(d,p) but shows a marked curvature for PM3. There is a good qualitative agreement between the shape of $V^{(2)}_{1,8}$ for all methods, even though the PM3-based approaches seem to be slightly flatter than MP2/SBK(d,p). Finally, we notice that in the case of $V^{(2)}_{1,10}$, the use of the MP2/SBK(d,p) normal modes enables the PM3 @ MP2/SBK(d,p) approach to recover some of the curvature of the potential, leading to a better description of this mode-mode coupling potential. Therefore, the composite PM3 @ MP2/SBK(d,p) approach displays a better *qualitative* agreement with MP2/SBK(d,p) coupling potentials than PM3 alone, even if the system is not sitting at its minimum geometry.

C. Application: Low-lying isomers of noradrenaline

1. Nature of the two isomers

Previous studies[1–3] have shown that noradrenaline has a large number of possible isomers. Van Mourik identified two low-lying isomers (AG1a and GG1a, see Ref. 3 for details of the nomenclature) as being particularly likely to be the ones observed in the gas-phase experiment of Snoek *et al.* In the present work, we use the MP2/TZP level of *ab initio* theory to investigate both AG1a and GG1a isomers. This electronic-correlation treatment has been found to be more reliable than density functional theory for this system due to the possibility of weak NH-π interactions.[1] Moreover, this particular combination of method and basis set leads to a good agreement between the computed CC-VSCF frequencies and the experimental data.[19] Figure 5 shows the optimized geometry of each isomer obtained at the MP2/TZP level.

We observe that both isomers have a similar total energy, $E_{\mathrm{tot}}(\mathrm{AG1a}) = -590.468\,514\,311\,5\ E_{\mathrm{h}}$ and $E_{\mathrm{tot}}(\mathrm{GG1a}) = -590.468\,526\,096\,6\ E_{\mathrm{h}}$. The energy dif-

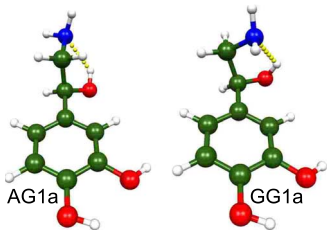

FIG. 5. (Color online) Minimum energy structures for the AG1a and GG1a conformers of noradrenaline obtained at the MP2/TZP level of theory.

TABLE II. Comparison of the direct fast-STA-CC-VSCF vibrational frequencies for the OH-stretch of two conformations of the noradrenaline molecule (AG1a and GG1a) calculated at the MP2/TZP *ab initio* level. The assignments of the normal modes are given in the last column. Experimental values are taken from Ref. 3. All frequencies are in cm^{-1}.

	Method							
	Harmonic		Diagonal		Fast-STA-CC-VSCF			
Mode	AG1a	GG1a	AG1a	GG1a	AG1a	GG1a	Experiment	
1	3887	3886	3721	3720	3672	3656	3669	$\tilde{\nu}_{OH_{free}}$
2	3834	3833	3665	3665	3638	3647	3614	$\tilde{\nu}_{OH\rightarrow OH}$
3	3734	3730	3551	3546	3531	3517	3527	$\tilde{\nu}_{OH\rightarrow NH_2}$
4	3670	3667	3738	3732	3495	3494	···	NH_2 asym.
5	3566	3562	3492	3488	3395	3402	···	NH_2 sym.

ference $E_{tot}(AG1a)-E_{tot}(GG1a)$ is $-0.011\,785\,1$ mE_h or ≈ -3 cm^{-1}, indicating that the GG1a isomer is the lowest-energy minimum at this level of theory. However, such energy difference is below the accuracy generally achieved by MP2 using triple-zeta basis sets [usually about 350–140 cm^{-1} (Ref. 35)], and thus these isomers have to be considered degenerate at this level of theory. In the optimized structures, the $-OH\cdots NH_2$ distance is 2.106 Å for AG1a and 2.116 Å for GG1a. These groups are close enough to each other to infer the presence of an intramolecular hydrogen bond between OH and NH_2 in both isomers, even if the bond angle is slightly outside the expected range[36] for a usual hydrogen bond (120.6° and 119.9° for AG1a and GG1a, respectively). The presence of this interaction has a direct impact on the vibrational frequency of the OH group concerned, leading to a redshift compared to a free OH-stretch frequency. We also observe the presence of a weaker intramolecular hydrogen bond between the catechol OH groups for each isomer. For AG1a, we find an $OH\cdots OH$ distance of 2.134 Å and an OHO hydrogen bond angle of 114.5°, and for the GG1a isomer a distance of 2.139 Å and OHO angle of 114.4°. Both of these slightly weaker hydrogen bonds lead to a small redshift in the OH-stretch frequency. We therefore expect to observe three transitions in the OH-stretch region: one relatively free OH-stretch frequency ($\tilde{\nu}_{OH_{free}}$), a slightly redshifted $OH\cdots OH$ stretch frequency ($\tilde{\nu}_{OH\rightarrow OH}$), and a moderately redshifted $OH\cdots NH_2$ stretch frequency ($\tilde{\nu}_{OH\rightarrow NH_2}$). However, the structures of these two isomers are very similar, with the only characteristic difference being the $\delta(N-C-C-O)$ torsion angle of the aminohydroxyethyl group (+52.0° for the AG1a isomer and −55.1° for GG1a). The torsion angles calculated by van Mourik and Früchtl[2] for AG1a and GG1a structures obtained at the MP2/6-31+G(*d*) level of theory are in good agreement with our MP2/TZP values. Following the labeling convention used by van Mourik and Früchtl, we obtain for AG1a $\delta(C_\gamma-C_\beta-C_\alpha-N)=+173.1°$ and $\delta(C_\gamma-C_\beta-O-H)$

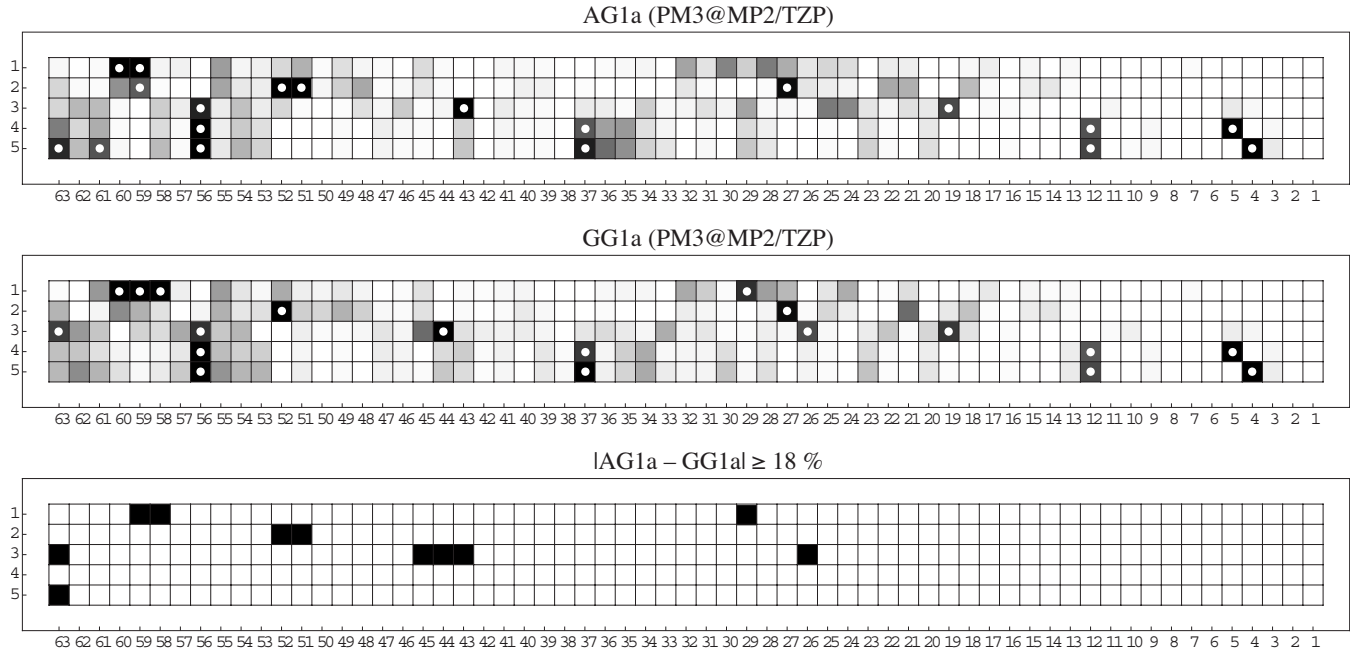

FIG. 6. Mode-mode coupling maps for AG1a (top) and GG1a (center) isomers of noradrenaline computed at the PM3@MP2/TVP level of theory. The bottom map shows couplings for which the absolute difference in coupling strength between AG1a and GG1a is greater than or equal to 18%.

TABLE III. Comparison of the frequency shift for the OH-stretch modes of two conformers of the noradrenaline molecule (AG1a and GG1a) calculated at the MP2/TZP *ab initio* level. Experimental values are taken from Ref. 3. All frequency differences are in cm^{-1}.

	Method						
	Harmonic		Diagonal		Fast-STA-CC-VSCF		
Difference	AG1a	GG1a	AG1a	GG1a	AG1a	GG1a	Experiment
$\tilde{\nu}_1-\tilde{\nu}_2$	53	53	56	55	34	9	55
$\tilde{\nu}_1-\tilde{\nu}_3$	153	156	170	174	141	139	142
$\tilde{\nu}_2-\tilde{\nu}_3$	100	103	114	119	107	130	87

$=-158.0°$ compared to $+173.8°$ and $-160.0°$, respectively. For GG1a, we compute $\delta(C_\gamma-C_\beta-C_\alpha-N)=+68.9°$ and $\delta(C_\gamma-C_\beta-O-H)=-87.0°$ compared to $+68.8°$ and $-88.7°$, respectively. The torsion angle in GG1a allows one proton of the $-NH_2$ group to interact weakly with the aromatic cycle to form a weak π-hydrogen bond (2.74 Å).

When comparing the different intramolecular hydrogen bonding situations for the OH groups of each isomer, we note that there is little difference between them and thus expect both AG1a and GG1a to have similar redshifts. Consequently, we suggest that the difference in the vibrational signature of these two isomers in the OH-stretch region originates from the change in mode-mode coupling pattern caused by the different torsion angles of the aminohydroxyethyl group in each isomer.

2. Vibrational study

The computed harmonic, diagonal and fast-STA-CC-VSCF vibrational frequencies for the OH-stretch and NH-stretch regions of each isomer are shown in Table II. We note that there is very little difference between the OH-stretch harmonic frequencies for AG1a and GG1a. The NH stretches, which are not observed experimentally due to their weak oscillator strength, are similar for both conformers (within 4 cm^{-1} of each other), despite the presence of a weak π-hydrogen interaction in GG1a. Such lack of differentiation at the harmonic level was also noted by van Mourik[1] for several levels of *ab initio* theory.

A diagonal approach to anharmonicity—taking $V_j^{(1)}(Q_j)$ into account but neglecting all mode-mode coupling—leads to an improvement in the overall agreement between the computed and the observed frequencies. However, we note that there is still very little difference between the computed diagonal frequencies of AG1a and GG1a. This indicates that a simple diagonal treatment of anharmonicity is not sufficient to explain the vibrational dynamics of this system.

The introduction of mode-mode coupling through the fast-STA-CC-VSCF method further improves the agreement between calculation and experiment. The 18 strongest mode-mode couplings are included in the calculation, for which $\zeta \geq 0.18\zeta_{max}$ are shown in Fig. 6 for each conformer. The reduced number of couplings leads to a calculation of the required PES that is 14 times faster than with the STA-CC-VSCF method, and 89 times faster than a full CC-VSCF calculation. Moreover, we now notice a difference between the computed OH-stretch frequencies of AG1a and those of GG1a. The mean difference between calculation and experiment for this part of the spectrum is 10 cm^{-1} for AG1a and 19 cm^{-1} for GG1a. It is interesting to compare the pattern of frequency shifts for the OH-stretch modes shown in Table III.

As observed earlier, both harmonic and diagonal models are unable to differentiate reliably between the two conformers. We see, however, that there is a reasonably good agreement between the harmonic frequency shifts and the shifts observed experimentally. The diagonal model provides a similar agreement for $\tilde{\nu}_1-\tilde{\nu}_2$ but overestimates $\tilde{\nu}_1-\tilde{\nu}_3$ and $\tilde{\nu}_2-\tilde{\nu}_3$.

The coupled model (fast-STA-CC-VSCF) shows that the frequency shifts obtained for the AG1a conformer are closer to the experimental values than those obtained for the GG1a conformer. Indeed, for this latter conformer, we see a closing of the $\tilde{\nu}_1-\tilde{\nu}_2$ gap and a widening of the $\tilde{\nu}_2-\tilde{\nu}_3$ separation. This is not the case for AG1a, which maintains a sizable gap between $\tilde{\nu}_1$ and $\tilde{\nu}_2$.

This observation, along with a better agreement between the fast-STA-CC-VSCF OH-stretch frequencies and experiment, leads us to suggest that AG1a is the conformer observed experimentally by Snoek *et al.*[3] It should be noted, however, that the main remit of the present study is to highlight the importance of mode-mode coupling in determining the vibrational signature of AG1a and GG1a rather than to perform a definitive calculation of the vibrational spectra of these two conformers.

The mode-mode coupling maps for each conformer shown in Fig. 6 shed some light on the differences between AG1a and GG1a that lead to a different vibrational signature in the OH-stretch region. We observe that both conformers have very similar coupling patterns and that the difference between them is relatively small: only a handful of mode-mode couplings are unique to each conformer. The largest differences (greater than or equal to 18%) are highlighted in the lowest panel of Fig. 6. An analysis of the normal modes involved reveals, as expected, that in each case the difference can be traced back to the position of the aminohydroxyethyl group and the presence of an intramolecular hydrogen bond. This also further justifies the need for an accurate representation of both the torsions and the hydrogen bonding in the PES, by using correlated methods with at least a triple-zeta basis set, in order to be able to describe the vibrational dynamics of these conformers realistically.

V. CONCLUSIONS

In this study, we have introduced a new type of reduced mode-mode coupling scheme, the fast-STA approach, that can be used to perform vibrational CC-VSCF calculations efficiently on a group of selected frequencies for large molecular systems. We have shown, using a set of five aliphatic alcohol molecules, that fast-STA-CC-VSCF is more accurate than the fast-CC-VSCF method for the selected frequencies and only marginally less accurate than the STA-CC-VSCF approach. Moreover, the accuracy of our approach can be improved at will by including more mode-mode couplings, at the expense of computational time. The fast-STA method leads to considerable time saving for the computation of the necessary PES compared to STA-CC-VSCF, fast-CC-VSCF, and full CC-VSCF techniques, being up to 115 times faster than the latter in the case of *n*-pentanol.

We have also investigated the issue of normal-mode matching that can occur when selecting mode-mode couplings using a low-level PES for systems that are sensitive to the level of theory used. We have showed that the use of high-level normal modes for the exploration of the low-level PES leads to a good qualitative agreement with the high-level mode-mode coupling map, thus bypassing the need for a problematic conversion between both sets of normal modes.

We performed *ab initio* MP2/TZP calculations for the two lowest conformers of noradrenaline, namely, AG1a and GG1a, and observed that they are energetically degenerate at this level of theory. The fast-STA-CC-VSCF method, along with our new approach to the computation of coupling maps, was then used to calculate the OH-stretch and NH-stretch frequencies of AG1a and GG1a. Our reduced-coupling approach allowed us to run the PES calculation 89 times faster than with the full CC-VSCF technique, thus making it possible to use a high-level MP2/TZP description of the PES. We saw that while both harmonic and diagonal approximations are unsatisfactory, the inclusion of the strong mode-mode couplings in the PES is able to lead to a differentiation of the OH-stretch vibrational frequencies of the AG1a and GG1a conformers. Our fast-STA-CC-VSCF results identify AG1a as the likely conformer observed in the experiments of Snoek *et al.*[3]

This study shows that the fast-STA-CC-VSCF method enables an efficient treatment of anharmonicity for large molecular systems, using high-level PESs, and that this method offers new perspectives for a better understanding of the intricate vibrational dynamics of biomolecules.

ACKNOWLEDGMENTS

D. M. Lauvergnat is acknowledged for helpful discussions. T. van Mourik is acknowledged for bringing this topic to our attention and performing some preliminary VSCF calculations on AG1a. R. C. Benoit is gratefully acknowledged for proof reading the manuscript. This work was supported by a grant (No. SFB-569/TP-N1) from the Deutsche Forschungsgemeinschaft (DFG).

[1] T. van Mourik, Chem. Phys. Lett. **414**, 364 (2005).
[2] T. van Mourik and H. A. Früchtl, Mol. Phys. **103**, 1641 (2005).
[3] L. C. Snoek, T. van Mourik, and J. P. Simons, Mol. Phys. **101**, 1239 (2003).
[4] T. F. Miller III and D. C. Clary, Mol. Phys. **103**, 1573 (2005).
[5] J. O. Jung and R. B. Gerber, J. Chem. Phys. **105**, 10332 (1996).
[6] D. M. Benoit, J. Chem. Phys. **120**, 562 (2004).
[7] O. Christiansen, J. Chem. Phys. **119**, 5773 (2003).
[8] K. Yagi, S. Hirata, and K. Hirao, J. Chem. Phys. **127**, 034111 (2007).
[9] K. M. Christoffel and J. M. Bowman, Chem. Phys. Lett. **85**, 220 (1982).
[10] S. Carter, J. M. Bowman, and N. C. Handy, Theor. Chem. Acc. **100**, 191 (1998).
[11] O. Christiansen, J. Chem. Phys. **120**, 2149 (2004).
[12] D. M. Benoit, J. Chem. Phys. **125**, 244110 (2006).
[13] G. C. Carney, L. L. Sprandel, and C. W. Kern, Adv. Chem. Phys. **37**, 305 (1978).
[14] J. M. Bowman, J. Chem. Phys. **68**, 608 (1978).
[15] N. J. Wright and R. B. Gerber, J. Chem. Phys. **112**, 2598 (2000).
[16] S. Carter, S. J. Culik, and J. M. Bowman, J. Chem. Phys. **107**, 10458 (1997).
[17] J. Kongsted and O. Christiansen, J. Chem. Phys. **125**, 124108 (2006).
[18] K. Yagi, T. Taketsugu, K. Hirao, and M. Gordon, J. Chem. Phys. **113**, 1005 (2000).
[19] G. M. Chaban, J. O. Jung, and R. B. Gerber, J. Chem. Phys. **111**, 1823 (1999).
[20] G. M. Chaban, J. O. Jung, and R. B. Gerber, J. Phys. Chem. A **104**, 10035 (2000).
[21] S. Irle and J. M. Bowman, J. Chem. Phys. **113**, 8401 (2000).
[22] J. M. Bowman, S. Carter, and X. Huang, Int. Rev. Phys. Chem. **22**, 533 (2003).
[23] L. S. Norris, M. A. Ratner, A. E. Roitberg, and R. B. Gerber, J. Chem. Phys. **105**, 11261 (1996).
[24] N. Matsunaga, G. M. Chaban, and R. B. Gerber, J. Chem. Phys. **117**, 3541 (2002).
[25] K. Yagi, S. Hirata, and K. Hirao, Phys. Chem. Chem. Phys. **10**, 1781 (2008).
[26] Y. Scribano and D. M. Benoit, J. Chem. Phys. **127**, 164118 (2007).
[27] M. Schmidt, K. Baldridge, J. Boatz, S. Elbert, M. Gordon, J. Jensen, S. Koseki, N. Matsunaga, K. Nguyen, S. Su, T. L. Windus, M. Dupuis, and J. A. Montgomery, J. Comput. Chem. **14**, 1347 (1993).
[28] W. J. Stevens, H. Basch, and M. Krauss, J. Chem. Phys. **81**, 6026 (1984).
[29] W. J. Stevens, M. Krauss, H. Basch, and P. G. Jasien, Can. J. Chem. **70**, 612 (1992).
[30] T. R. Cundari and W. J. Stevens, J. Chem. Phys. **98**, 5555 (1993).
[31] T. H. Dunning, Jr., J. Chem. Phys. **55**, 716 (1971).
[32] G. Rauhut, J. Chem. Phys. **121**, 9313 (2004).
[33] K. Yagi, S. Hirata, and K. Hirao, Theor. Chem. Acc. **118**, 681 (2007).
[34] S. Heislbetz, P. Schwerdtfeger, and G. Rauhut, Mol. Phys. **105**, 1385 (2007).
[35] S. E. Barrows, J. W. Storer, C. J. Cramer, A. D. French, and D. G. Truhlar, J. Comput. Chem. **19**, 1111 (1998).
[36] G. A. Jeffrey, *An Introduction to Hydrogen Bonding* (Oxford University Press, New York, 1997).